A Novel Double Layered Weighted Potential Field Framework for Multi-USV Navigation towards Dynamic Obstacle Avoidance in a Constrained Maritime Environment

Tamzidul Mina[1, 2], Yogang Singh[1], and Byung-Cheol Min[1]

[1]SMART Lab, Department of Computer and Information Technology, Purdue University, IN 47907, USA
[2]School of Mechanical Engineering, Purdue University, IN 47907, USA

***Abstract*—Motion planning of multiple unmanned surface vehicles (USVs) towards increased autonomy and wider coverage of the maritime environment is a pertinent requirement. Given the numerous types of USVs currently available with a wide spectrum of maneuvering capabilities, we present a generalized multi-USV navigation framework adaptable to specific USV maneuvering response capabilities for dynamic obstacle avoidance. The present paper integrates an optimal path planning with safety distance constrained A* algorithm and a proposed adaptively weighted potential field based path following approach with collision avoidance based on USV maneuvering response times. The system allows USVs with fast maneuvering abilities to react late and slow USVs to react sooner to oncoming moving obstacles gradually such that a smooth path is followed by the USV group with reduced cross track error. Simulation results validate reduced cross track error for slow and fast maneuvering response time multi-USV teams.**

***Keywords*—Multi-Vehicle Systems, Path Planning, Unmanned Surface Vehicles, Weighted Potential Function**

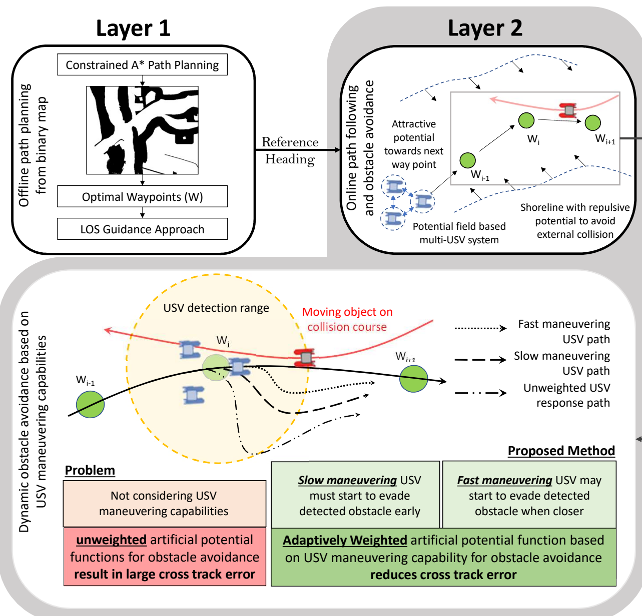

Figure 1: Conceptual illustration of the double layered weighted potential function framework for multi-USV navigation based on USV maneuvering capabilities to reduce cross track error. Layer 1 generates a path from a given map and layer 2 implements path following with adaptively weighted collision avoidance and inter-USV dynamics.

I. Introduction

With increasing demand of autonomous systems in maritime environment, the application of Unmanned Surface Vehicles (USVs) has gained a lot of momentum in the last few decades. High performance marine vehicles operating in maritime environment are employed in various applications such as bathymetric surveys, ocean monitoring, and data acquisition [1], [2].

Substantial research has been conducted towards increasing the intelligence of USVs with autonomous ships being the basis of the research motivation [3]. Recent works have focused on moving multiple USVs as a team to improve the overall performance in terms of safety and implementation. As such, we stress two important areas of research on multi-USV systems; self-organization including formation control, and path planning and path following with obstacle avoidance in marine environments.

As representative works on multi-USV self-organization and formation control, we highlight behavior-based multi-agent interactions proposed in [4], [5], leader-follower approaches studied in [6], [7], and bio-inspired self-organization approaches for multi-agent systems in [8], [9]. An overview of the research work on the topic can be found summarized in [10], [11], [12], [13]. Recent works on path planning and real-time obstacle avoidance using Convention on the International Regulations for Preventing Collisions (COLREGS) without relying on LiDAR or other sensors have been proposed in [14]. Wang *et al.* proposed a hybrid approach combining A* algorithm path planning with Dynamic Window for obstacle detection and avoidance in the maritime environment. Recent studies on multi-USV path planning also include methods developed from bee colony dynamics [15] and computation time improvements using fast marching algorithms [16].

Artificial potential based approaches have been a popular choice for multi-agent self-organization, path following and obstacle avoidance [17]. An improved artificial potential field method specifically for USV obstacle avoidance have been recently proposed in [18]. An application specific research work on cooperative searching applications using multi-USV systems was presented in [19]. A USV navigation method using path planning with A* algorithm and collision probability distribution modeled by artificial potential fields was proposed in [20].

Although a lot of multi-USV path planning and obstacle avoidance research has been proposed in literature, very few has addressed applicability concerns of their proposed method on the wide variety of USVs currently available. USVs generally used by the military on surveillance and patrolling applications have high speed capabilities while USVs used for surveys, measurement or water monitoring tasks operate at slower speeds [21], [22]. USV shapes such as the Catamaran type include the Springer [23], [24], MIT's AutoCat [25] and Charlie [26]. Kayak type USVs have also been developed at MIT for autonomous surface missions [27]. Low cost small USVs have also been developed for specific purposes as presented in [28]. Most of the path following and obstacle avoidance methods proposed in literature are built on assumptions of specific capabilities of the modeled USVs, and fall short in generalizing their methods to these diverse shapes, weights, sizes, propulsion methods of USVs resulting in different maneuvering capabilities.

Therefore, in this paper we propose a novel generalized multi-USV navigation framework adaptable for different types of USV platforms. A constrained A* algorithm is used to define an optimal path with safety distance considerations from static obstacles in the environment. An adaptive weighting model based on a generalized USV maneuvering response time unit is presented that configures artificial potential terms in the system framework governing inter-USV, USV with moving obstacle and way point following interactions of attraction and repulsion, and adapts the framework to the USV maneuvering capabilities to allow improved path following performance for navigation in terms of reduced cross track error.

II. Problem Statement

We consider a fully connected leader-follower group of n USVs on a planar surface $\mathscr{W}$, each denoted as R_i, for $i \in I_R = \{1,2,..,n\}$ with position and orientation defined as $r_i = [x_i, y_i]$ and θ_i. Dynamics of each USV is modeled as an unicycle model,

$$\begin{aligned} \dot{x}_i &= v_i \cos\theta_i & \dot{v}_i &= a_i \\ \dot{y}_i &= v_i \sin\theta_i & \dot{\theta}_i &= \omega_i \end{aligned} \tag{1}$$

where v_i and $\dot{\theta}_i$ the linear and angular velocity of R_i. The control inputs of R_i are defined as $[u_i, w_i]$, where $u_i = a_i$ and $w_i = \omega_i$. Referring to previous works on radar and LiDAR based obstacle detection for USVs [29], [30], we assume that all USVs have a circular field of view (FOV) of radius d centered at (x_i, y_i) for simplicity, within which it is able to detect moving and static obstacles. The group leader is denoted as R_h, where $h \in I_R$.

Given the wide variety of USVs currently available in the field, we consider a generalized *maneuvering response time unit* for R_i as t_r dependent on its size, weight, maximum speed, braking and various other factors for dynamic obstacle avoidance. We denote moving obstacles in $\mathscr{W}$ as M_i, for $i \in I_M = \{1,2,..,P_m\}$ with position m_i and stationary obstacles on the plane as O_i, for $i \in I_O = \{1,2,..,P_o\}$ with position o_i.

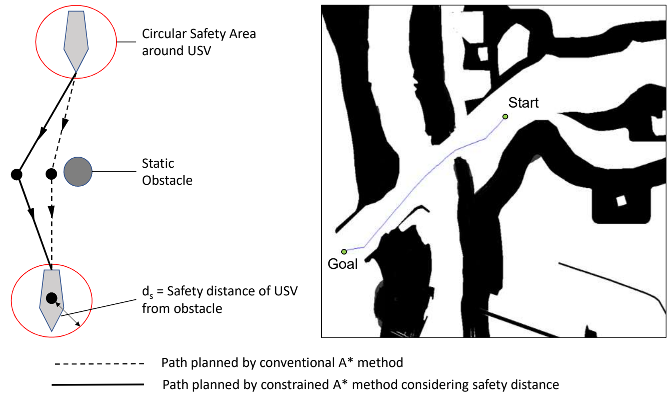

Figure 2: Schematic of the path generated from the path planner in Layer 1 (left) in [31] and the generated path on the map of Monterey Bay harbor (right).

The objective is for all n USVs to safely navigate through a given environment following an optimally generated path, aggregating and avoiding moving obstacles using our proposed adaptively weighted potential function framework based on USV maneuvering response time t_r for reducing cross track error.

III. Proposed Solution

The proposed generalized multi-USV navigation framework with dynamic obstacle avoidance in a constrained environment consists of two layers. On the top level of the hierarchy (layer 1), a robust path planner based on constrained A* approach [31] is adopted to generate optimal way points, which are used to generate reference heading for guidance using the line-of-sight (LOS) method. The reference heading is fed into the lower hierarchy (layer 2) of online path following based on a proposed adaptively weighted artificial potential function framework for USV interaction, obstacle avoidance and navigation. The novelty of the study lies in this level where the potential function terms of inter-USV interaction, way point attraction and moving obstacle avoidance are adaptively weighted based on USV maneuvering response times to reduce cross track error during dynamic collision avoidance, while navigating in an environment with moving vessels. Fig. 1 shows the schematic of the double layered hybrid framework for the multi-USV system.

A. Constrained A* offline Path Planning

In this study, a computationally efficient constrained A* approach has been adopted towards offline path planning for the multi-USV group from [31] to form layer 1 of the proposed multi-USV framework. In this layer, a safety distance constrained A* approach, where the USV is enclosed by a certain safety distance d_s, is applied to determine the way points for navigation. The adopted A* approach in this study considers a circle enclosing the USV as safety distance, as shown in Fig. 2 (left). We denote the way points generated by the proposed approach as w_i, for $i \in I_W = \{1,2,..,P_w\}$ in order.

B. Online Path Following with Dynamic Obstacle Avoidance

1) Weighted potential functions: We define a set of artificial potential functions to model a leader-follower based multi-USV system interacting with its environment,

$$U_{r_i}^{r_j}(r_i,r_j) = \frac{1}{2}\eta_{11}\left(\ln||r_i - r_j|| + \frac{d_{ij}}{||r_i - r_j||}\right) + \frac{1}{2}\eta_{12}(||r_i - r_j|| - d_{ij})^2, \qquad i,j \in I_R \quad (2)$$

$$U_{r_h}^{w_p}(r_h,w_p) = \frac{1}{2}\eta_2||r_h - w_p||^2, \qquad h \in I_R, p \in I_W \quad (3)$$

$$U_{r_i}^{m_k}(r_i,m_k) = \frac{1}{2}\eta_3\left(||r_i - m_k|| - d\right)^2, \qquad i \in I_R, k \in I_M \quad (4)$$

$$U_{r_i}^{o_l}(r_i,o_l) = \frac{1}{2}\eta_4\left(\frac{1}{||r_i - o_l||} - \frac{1}{d_{io}}\right)^2, \qquad i \in I_R, l \in I_O \quad (5)$$

where η_{11}, η_{12}, η_2, η_3 and η_4 are positive scaling constants for their corresponding potential functions.

Artificial potential function $U_{r_i}^{r_j}$ models inter-USV interaction as a function of the relative distance between pairs of USVs R_i and R_j, with an equilibrium distance of d_{ij}. The leader USV R_h is unaffected by the interaction of the follower USVs in the group, while the follower USVs are affected by the leader and all other USVs to form a leader-follower type swarm aggregation model.

Each optimal way point w_i, for $i \in I_W = \{1,2,..,P_w\}$ obtained from path planning on the top layer acts as an intermediate goal point having an attractive potential. The function $U_{r_h}^{w_p}$ models the attraction of leader R_h towards the next way point location w_p on the path as a function of the relative distance between r_h and w_p. This leads to traversing of the multi-USV system towards a final goal point cutting across intermediate way points.

We consider collision avoidance of USVs from moving obstacles in the environment as a repulsive potential. The potential function $U_{r_i}^{m_k}$ models the interaction of R_i with a detected moving obstacle m_k within radius d, as a function of the relative distance between r_i and m_k for dynamic obstacle avoidance.

The function $U_{r_i}^{o_l}$ models the repulsive interaction of R_i with detected static obstacles o_l with influence distance d_{io}, as a function of the relative distance between r_i and o_l. This ensures collision avoidance with static objects (shoreline, anchored vessels) in constrained channels of maritime environments. We assume that at initial time, $\|r_i - r_j\|$, $\|r_h - w_p\|$, $\|r_i - m_k\|$ and $\|r_i - o_l\|$ are all non-zero terms.

We accommodate the applicability of our framework to various types of multi-USV teams by proposing a weighting scheme for the aforementioned set of potential functions based on USVs having different maneuverability response times. We consider a scenario where a multi-USV team following a trajectory is on a collision course with a moving object detected within d. For a multi-USV team capable of fast maneuvering (fast response times), collision avoidance could be prioritized

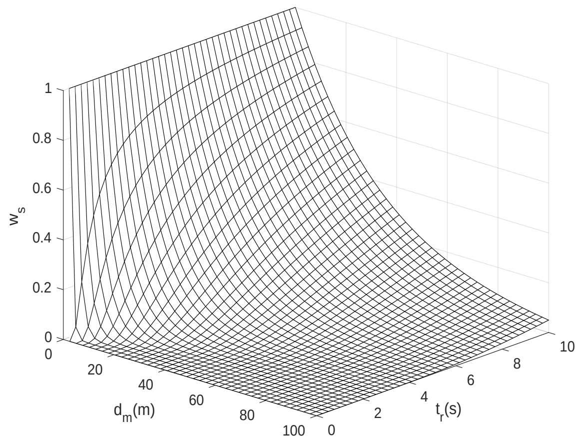

Figure 3: Adaptive weighting model based on moving obstacle distance d_m and USV maneuvering response time t_r, for $K_w = 0.25$.

much later when the object is closer; the multi-USV team may prioritize minimizing cross track error and maintaining inter-USV distances until then. However, for a multi-USV team having slow maneuvering capabilities, collision avoidance must be prioritized sooner to allow enough time for maneuvering, over minimizing cross track error and maintaining inter-USV distances. Thus, we model the weighted potential function of R_i as,

$$U_w(r_i,r_j,r_h,w_p,m_k,o_l) = (1-w_s)\left[\sum_{j\neq i, i\neq h} U_{r_i}^{r_j} + U_{r_h}^{w_p}\right] + w_s\sum U_{r_i}^{m_k} + \sum U_{r_i}^{o_l} \quad (6)$$

where $w_s \in (0,1)$ is the weighting term dependant on USV maneuvering capabilities quantified as maneuvering response time t_r. The resultant force on R_i is therefore,

$$F_i(r_i,r_j,r_h,w_p,m_k,o_l) = (1-w_s)\left[\sum_{j\neq i, i\neq h} \nabla U_{r_i}^{r_j} + \nabla U_{r_h}^{w_p}\right] - w_s\sum \nabla U_{r_i}^{m_k} - \sum \nabla U_{r_i}^{o_l}. \quad (7)$$

The target orientation of R_i in the next time step is set consistent with the direction of F_i and the magnitude of the resultant control input denoted as $||F_i||$ is utilized as the control u_i in Eq. (1).

2) Adaptive weighting model based on USV maneuverability response times: An exponential based adaptive weighting model is proposed to accommodate USVs with different maneuverability response times t_r in relation to distance to the detected moving object $d_m = \|r_i - m_k\|$,

$$w_s = e^{-\frac{K_w d_m}{t_r}} \quad (8)$$

where K_w is a positive scaling constant for $w_s \in (0,1)$.

Figure 3 illustrates the resulting relationship of w_s with $0 < d_m(m) \leq 100$, $0 < t_r(s) \leq 10$ and $K_w = 0.25$. For large t_r, a higher weighting w_s is obtained over decreasing d_m. In contrast, for low t_r cases, weighting w_s remains relatively low at higher d_m but quickly increases at lower d_m.

We justify our choice of an exponential based weighting model to allow a slow change in w_s for larger values of d_m at any particular t_r. As d_m gets smaller the rate of change in w_s gradually increases, until rapidly reaching its upper bound infinitesimally close to distance d_m of zero. We utilize these characteristics of the exponential function to create a reduced cross track error path following scheme for the USV group on a collision course with a moving obstacle.

C. Controller Analysis

The artificial potential function based multi-USV system proposed in this paper is based on the leader-follower type swarm aggregation concept [32]. The elected group leader is attracted to way points on the path sequentially, and is unaffected by the following group's inter-USV interactions; whereas all followers are affected by the leader and all other USVs on the group. The artificial potential function in Eq. (2) describing the inter-USV interaction ensures the aggregation of all USVs, keeping them in close proximity to each other.

We first analyze the convergence of the USVs to inter-USV equilibrium distance d_{ij} without the leader USV being affected by the followers, and no inter-USV collisions. To investigate the stability and the convergence of the multi-USV system to equilibrium inter-agent distance d_{ij} using the proposed control law, we define the Lyapunov function as,

$$V(r,v) = U(r) + \frac{1}{2}v^{\mathrm{T}}v \tag{9}$$

where $r \in \mathbb{R}^{ns}$ and $v \in \mathbb{R}^{ns}$ are stacked position and velocity vectors of n robots in the system, and $U(r) : \mathbb{R}^{ns} \longrightarrow \mathbb{R}_{>0}$ is the collective potential energy of the system written as,

$$U(r) = \sum_{i=1, i\neq h}^{n} \sum_{j\neq i}^{n} U_{r_i}^{r_j}(\|r_i - r_j\|). \tag{10}$$

The collective dynamics of the multi-USV system is written as,

$$\dot{r} = v, \qquad \dot{v} = -\nabla U(r) - \hat{L}(r)v \tag{11}$$

where $\hat{L}(r)$ is the Kronecker product of the fully connected multi-USV system's graph Laplacian $L(r)$ and identity matrix I_p.

Proof. We differentiate $V(r,v)$ and substitute Eq. (11):

$$\begin{aligned}\dot{V}(r,v) &= \dot{r}^T \nabla U(r) + v^T \dot{v} \\ &= v^T \nabla U(r) + v^T(-\nabla U(r) - \hat{L}(r)v) \\ &= -v^T \hat{L}(r) v \leq 0. \end{aligned} \tag{12}$$

Therefore, using LaSalle's Invariance Principle, we conclude that velocities of all follower USVs will converge, i.e., $\forall i \neq h, j : v_i = v_j$. With the total system energy bounded $V(r,v) \leq C$, the velocities are bounded as well $\|v\| \leq \sqrt{2C}$. Bounded and matching velocities imply that inter-USV distances remain constant, $\forall i \neq h, j : \|r_i - r_j\| = 0$. Hence,

$$\dot{U}(r) = \sum_{i=1, i\neq h}^{n} \sum_{j\neq i}^{n} (\dot{r}_i - \dot{r}_j)^T \nabla U_{r_i}^{r_j}(\|r_i - r_j\|) = 0 \tag{13}$$

implying that $U(r)$ is constant at steady state. Moreover, we also conclude $\dot{v} = -\nabla U(r)$, since $\hat{L}(r)v = 0$ due to matching velocities. With $\nabla U(r)$ as zero, the system reaches a local minimum with no change in USV velocities.

With initial conditions previously defined as $\|r_i - r_j\| \neq 0$, we also conclude that no inter-USV collision occurs in the system, since $\|r_i - r_j\| = 0$ causes $U(r) \longrightarrow \infty$ which contradicts $V(r,v) \leq C$. ■

The follower USV group's centroid is defined as,

$$\bar{r} = \frac{1}{n-1} \sum_{i=1, i\neq h}^{n-1} r_i. \tag{14}$$

The leader R_h is attracted to the next way point on the path defined by the attractive artificial potential $U_{r_h}^{w_p}(r_h, w_p)$ in Eq. (3). This net movement of R_h creates an asymmetry in the inter-USV interaction forces defined by the artificial potential function $U_{r_i}^{r_h}(r_i, r_h)$, resulting in the motion of the USV group.

Lemma 3.1: A group of $n-1$ follower USVs and 1 leader with dynamics defined as Eq. (1), and leader-follower and follower-follower USV dynamics defined as Eq. (6), the follower USV group's centroid dynamics are governed by the leader USV's attraction and repulsion,

$$\dot{\bar{r}} = -\frac{1}{n-1} \sum_{i=1, i\neq h}^{n-1} F_{r_i}^{r_h}(\|r_i - r_h\|)(r_i - r_h) \tag{15}$$

where $F_{r_i}^{r_h}$ denotes the interaction force between R_i and R_h.

Proof. Substituting the USV dynamics and inter-USV control law from Eq. (7) in the derivative of the follower USV group centroid expression in Eq. (14),

$$\begin{aligned}\dot{\bar{r}} &= \frac{1}{n-1} \sum_{i=1, i\neq h}^{n-1} \dot{r}_i \\ &= -\frac{1}{n-1} \sum_{i=1, i\neq h}^{n-1} \sum_{j=1, j\neq h}^{n-1} F_{r_i}^{r_j}(\|r_i - r_j\|)(r_i - r_j) \\ &\quad - \frac{1}{n-1} \sum_{i=1, i\neq h}^{n-1} F_{r_i}^{r_h}(\|r_i - r_h\|)(r_i - r_h). \end{aligned} \tag{16}$$

Since $F_{r_i}^{r_j}(\|r_i - r_j\|) = F_{r_j}^{r_i}(\|r_j - r_i\|)$, we reorganize the summation limits to obtain,

$$\begin{aligned}&\frac{1}{n-1} \sum_{i=1, i\neq h}^{n-1} \sum_{j=1, j\neq h}^{n-1} F_{r_i}^{r_j}(\|r_i - r_j\|)(r_i - r_j) \\ =&\frac{1}{n-1} \sum_{i=1, i\neq h}^{n-2} \sum_{j=i, j\neq h}^{n-1} [F_{r_i}^{r_j}(\|r_i - r_j\|)(r_i - r_j) \\ &+ F_{r_j}^{r_i}(\|r_j - r_i\|)(r_j - r_i)] = 0. \end{aligned}$$

Therefore, the first term in Eq. (16) governing the follower-follower USV attraction and repulsion equals 0, proving that Eq. (15) holds true. ■

The adaptive weighting model defines $ws \in (0,1)$. Thus, the inter-USV artificial potential based interaction term in Eq. (6) weighted by $1 - w_s$ never goes to zero. The USVs are also increasingly repelled by moving obstacles getting closer in the distance interval $[d, 0)$, i.e. the artificial potential based moving object repulsion term in Eq. (6) weighted by w_s is never zero. The USVs are also repelled by all static obstacles within d. Therefore, the aforementioned proofs hold such that no inter-USV collision occurs and all USVs in the system aggregate to the defined leader USV R_h in finite time. Since the leader R_h is attracted to the next way point on the path, we conclude that all USVs in the group converge to consecutive way points as well.

IV. Validation and Results

A. Setup

To validate our proposed method, we show that groups of n USVs having different maneuverability response times t_r, initially placed at a starting location of a given set of way points in a constrained channel, navigates along the way points successfully avoiding collision with moving objects in its path while reducing cross track error.

Monterey Bay has significant geological and topological importance, leading to the choice of the environment for the current study. A $694 \times 10{,}939$ pixel binary map of Monterey Bay with 1 pixel equivalent to $3.6m$ is used to generate a path along the constrained channel. The constrained A* algorithm used $72m$ as safety distance to generate the USV enclosing circle, based on the International Maritime Organisation (IMO) guidelines for collision avoidance in inland water ways. The generated path is shown in Fig. 2 (right) with the identified start and the goal points and is utilized as the set of way points for the simulations.

We set up the validation process with $n = 3$ and $n = 6$ robots having maneuverability response times of $t_r = 2$ and $t_r = 8$ in separate simulation scenarios. The maneuvering response times are modeled by tuning the low level orientation and speed controllers of each of the USVs to reflect the two t_r cases. A fast moving object is simulated approaching from the opposite direction. For each scenario, we compare the cross track error of the robot group following the path with and without using our proposed adaptively weighted potential function framework, to show that the resulting cross track error is significantly less using our proposed framework.

For brevity of simulations, we exaggerate the maximum allowed USV velocity to $7m/s$ and $5m/s$ in separate instances and the constant velocity of the moving object approaching from the opposite direction on a collision course as $8m/s$.

B. Experiment and Results

Figure 5 illustrates the comparison of the artificial potential function framework with and without adaptive weighting for $n = 3$ USVs, maneuvering response time $t_r = 2$. The time lapse comparison of the path followed by the USV group with and without the adaptive weighting framework as seen in Fig. 5a visually demonstrates the effectiveness of the adaptive weighting framework. The USV group having a fast maneuvering response time of $t_r = 2$ reacts much later to the oncoming moving object after detection, and thus successfully stays on its prescribed path with minor deviations with the adaptive weighted framework; whereas the USV group without

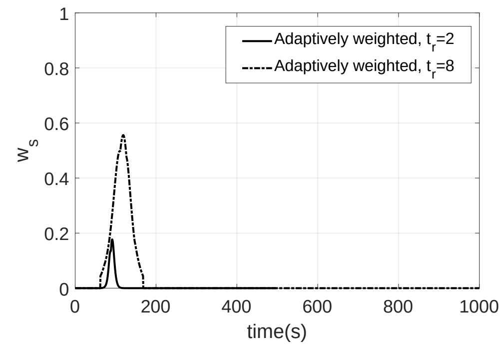

Figure 4: Adaptive weighting w_s with time for $n = 3$ robots, $t_r = 2$ and $t_r = 8$.

the framework drifts wide off course away from the oncoming moving object regardless of having a fast maneuvering response time.

In the unweighted case for maintaining inter-agent distance, way point following and moving obstacle avoidance, all USVs experienced strong repulsion from the moving obstacle with a strong tendency to stay in formation. Thus, the USV with the strongest repulsion from the moving obstacle strongly pulled the entire USV team along with it to move further away from the path. This phenomenon is observed as the large cross track error as shown in Fig. 5b.

In comparison, the adaptive weighting system allowed loose inter-USV interaction and way point following when near the fast moving obstacle so that individual USVs could avoid the moving obstacle without strongly influencing the team. The adaptive weighting for the fast response time $t_r = 2$ USV system also weighed moving object avoidance less until much closer to the object allowing USVs to stay on the path longer even after detection of the moving object on the path as shown in Fig. 5e. Thus, a smaller cross track error is observed with the proposed adaptive weighting APF framework as seen in Fig. 5b, while passing within a much smaller distance close to the $72m$ safety distance previously set with the adaptively weighted case while remaining. Fig. 5c shows the relevant plot of USV-object inter-distance over the simulation period. Figure 4 shows the obtained w_s profile with the adaptive weighting framework, and the corresponding inter-USV interaction force is shown in Fig. 5d. The magnitude of the inter-USV interaction forces was smaller for the adaptively weighted framework as expected with lower weighting when near a moving object, compared to the unweighted framework.

The simulation with $n = 3$ USVs, is repeated with maneuvering response time $t_r = 8$ and the USV group path following time lapse and resulting plots are shown in Fig. 6. Similar qualitative path following results to the $t_r = 2$ scenario was obtained with the $t_r = 8$ simulation case. The USV group having a slow maneuvering response time of $t_r = 8$ reacts relatively early to the oncoming object but gradually, proportional to the slowly increasingly weight w_s. The USV group successfully stays close to its prescribed path with minor deviations using the adaptive weighted framework; whereas

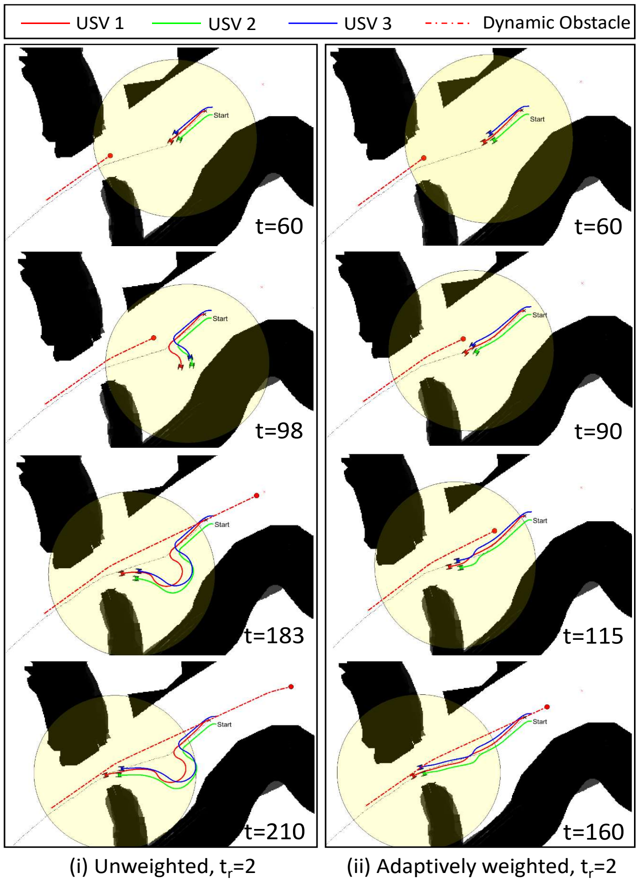

(a) Time lapse comparison for unweighted and adaptively weighted potential function based path following and obstacle avoidance.

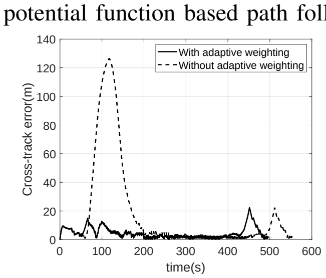

(b) Cross-track error comparison with time.

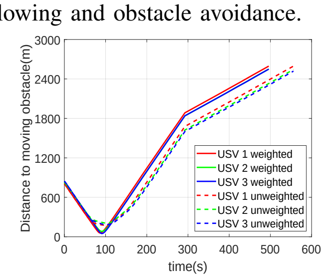

(c) USV to moving object distance with time.

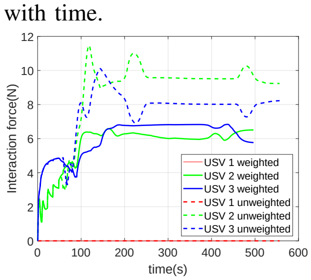

(d) Inter-agent interaction force with time.

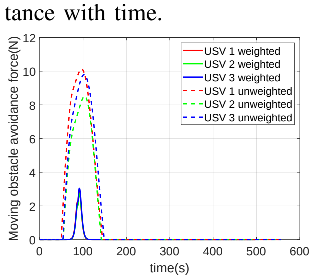

(e) Moving object and USV interaction force with time.

Figure 5: Simulation result for $n = 3$ robots, $t_r = 2$, on a collision course with a moving obstacle showing reduced cross track error with the adaptively weighted potential framework.

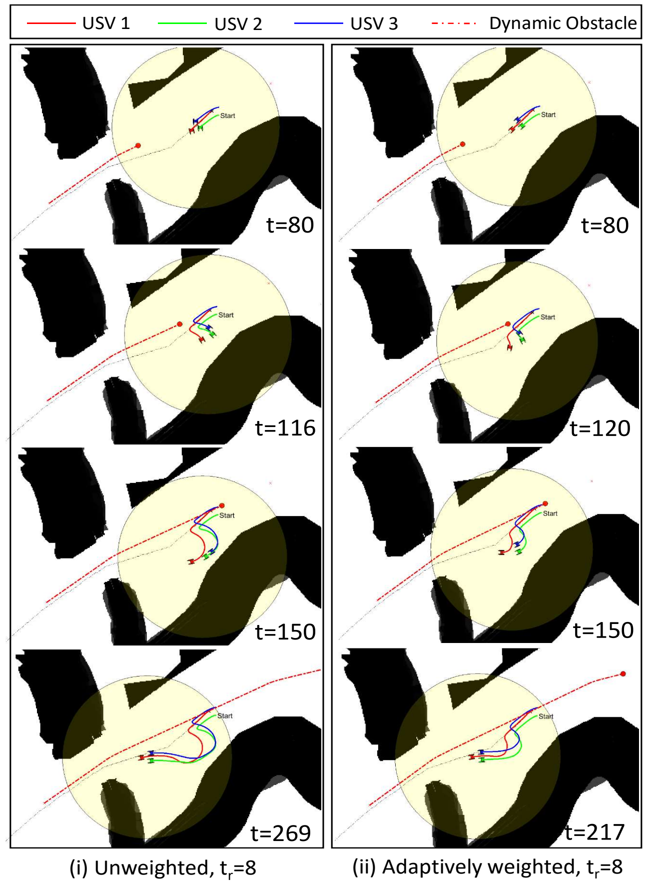

(a) Time lapse comparison for unweighted and adaptively weighted potential function based path following and obstacle avoidance.

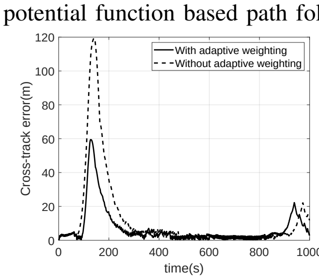

(b) Cross-track error comparison with time.

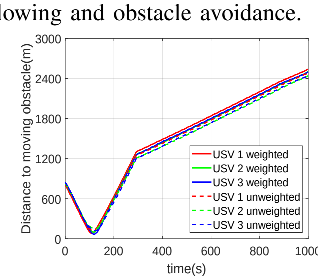

(c) USV to moving object distance with time.

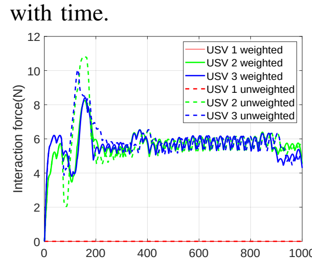

(d) Inter-agent interaction force with time.

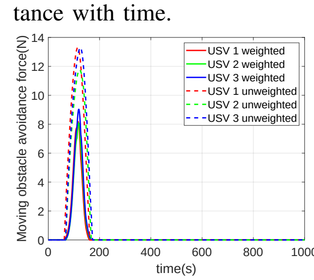

(e) Moving object and USV interaction force with time.

Figure 6: Simulation result for $n = 3$ robots, $t_r = 8$, on a collision course with a moving obstacle showing reduced cross track error with the adaptively weighted potential framework.

the USV group without the adaptive weighting framework starts to maneuver wide off course rapidly as soon as a moving object is detected in front. As a result, a large cross track error is observed without using the proposed adaptive weighting framework as seen in Fig. 6b. Here we also note that, due to the slow maneuvering response time $t_r = 8$, the cross track error was smaller than the cross track error obtained for the $t_r = 2$ case. A consistent pattern in the USV distance to moving object for $t_r = 8$ with the $t_r = 2$ case was obtained as shown in Fig. 6c.

With a slow maneuvering response time, the proposed adaptive weighting framework gradually moved the USV group away from the path of the moving object. This is evident from Fig. 4 where a higher w_s weight is reached for $t_r = 8$ over a longer period of time compared to $t_r = 2$. The plot shown in Fig. 6e verifies this finding that the interaction between the USV group and the moving object spanned a longer period of time and reached a higher peak for slow maneuvering response time $t_r = 8$, compared to the fast maneuvering case shown in Fig. 5e adhering to the modeled w_s function in Section III-B2. Using the adaptive weighting potential framework, the USV group remained much closer to the object and its defined path but greater than the safe distance previously set, compared to the unweighted case.

We repeat the maneuvering response time $t_r = 2$ and $t_r = 8$ simulation scenarios for $n = 6$ robots to present the effects of larger n, acknowledging the fact that only a small number of USVs may be appropriate in the group at once, due to spatial and operational constraints in a narrow channel marine environment.

The observations made for the $n = 6$ USV system were consistent with the $n = 3$ USV case. With the proposed adaptively weighted potential function framework, the fast maneuvering response time case resulted in a low peak and short time spanning w_s profile and the slow maneuvering response time case resulted a higher peak, and interaction spanning over a longer period of time as shown in Fig. 7. The magnitude of the inter-USV forces was smaller for the adaptively weighted framework as expected with lower weighting when near a moving object, compared to the unweighted framework in both cases of $t_r = 2$ and $t_r = 8$ shown in Fig. 8d and Fig. 9d.

For this $n = 6$ robot case, the slow maneuvering USV group with $t_r = 8$ showed higher magnitude in inter-USV forces even after interaction with the moving object has taken place. From the time lapse image we see that R_h has moved ahead much further leaving the follower USV group back due to the lower cross track error of the group, and strong inter-USV interactions within the follower USVs in the adaptively weighted potential function framework. Due to the attractive force of the follower USVs towards R_h, a higher magnitude inter-USV plots are observed for the proposed system. The w_s profiles for the two maneuvering response time cases are concordant with the USV and moving object interaction force plots with time for the two cases shown in Fig. 8e and Fig. 9e, showing a wider interaction region for the slower response time system compared to the fast response time

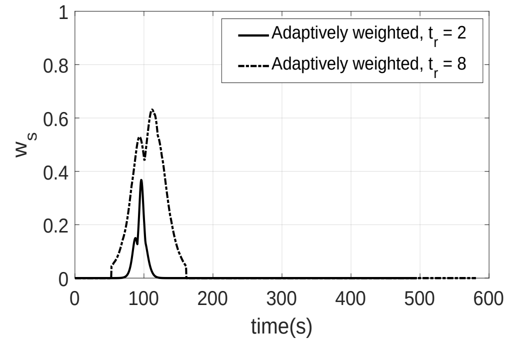

Figure 7: Adaptive weighting w_s with time for $n = 6$ robots, $t_r = 2$ and $t_r = 8$.

system. Both the cases exhibited a gradually growing slope in contrast to the unweighted system that consistently showed even larger USV and moving object interaction forces with rapid growth and spanning over a wider period of time for both the $t_r = 2$ and $t_r = 8$ cases respectively. As a result, the performance comparison for a $n = 6$ USV group with and without the proposed adaptively weighted potential function framework, for both fast and slow maneuvering response times exhibited significantly less cross tracking error with the proposed adaptively weighted potential function framework compared to the unweighted system in separate simulation instances as seen in Fig. 8b and Fig. 9b. Similar to the $n = 3$ USV case, the USV group passed the moving object with the minimum recorded distance just above the safety distance set at $72m$ with the adaptively weighted case. In comparison, the unweighted case resulted in the USV group following a much wider path around the moving object for both cases of $t_r = 2$ and $t_r = 8$ as seen in Fig. 8c and Fig. 9c.

Potential function based systems operate relying on the overall energy state of the system. The system tends to move towards the closest minimum energy state termed as the equilibrium condition. For increasing n, the total energy of the system is higher and depending on the difference between the initial system potential energy state and equilibrium state, the rate at which the system tends to move towards equilibrium is also higher. Therefore, the scaling parameters for the potential functions must be tuned appropriately for significant changes in n.

A video of the simulations is available for reference at http://smart-laboratory.org/docs/oceans19-wpf.mp4.

V. Conclusion

In this paper, a novel multi-USV navigation framework with path planning and adaptively weighted potential functions for dynamics obstacle avoidance with reduced cross track error based on various maneuvering response time capabilities of various USV systems is proposed. The system adaptively weights inter-USV interactions, USV and moving object repulsion, and leader attraction to the next way point to improve path following performance of multi-USV teams on a collision course with a moving object. The path followed to avoid dynamic obstacles offer less drastic cornering for USVs using

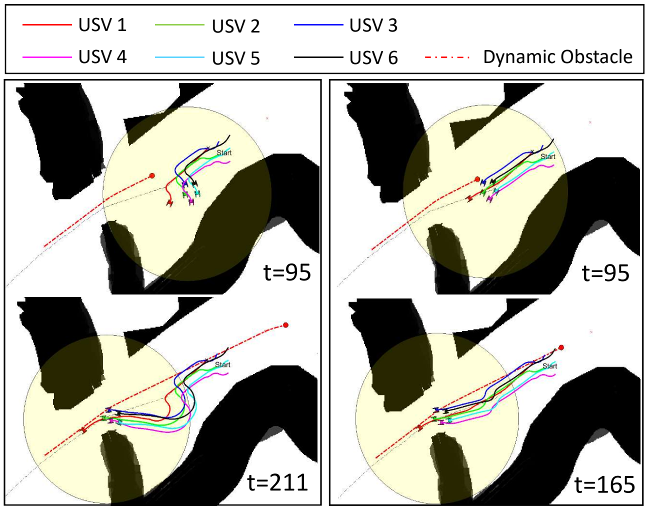

(i) Unweighted, t_r=2 (ii) Adaptively weighted, t_r=2

(a) Time lapse comparison for unweighted and adaptively weighted potential function based path following and obstacle avoidance.

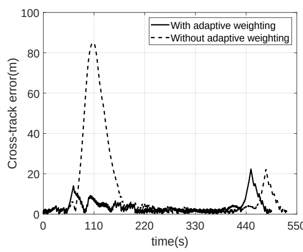

(b) Cross-track error comparison with time.

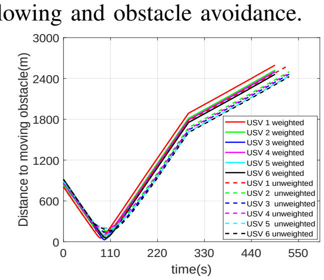

(c) USV to moving object distance with time.

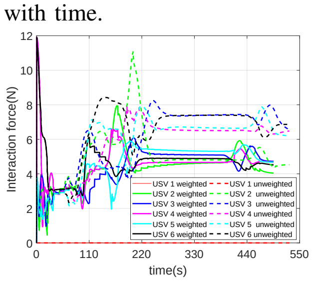

(d) Inter-agent interaction force with time.

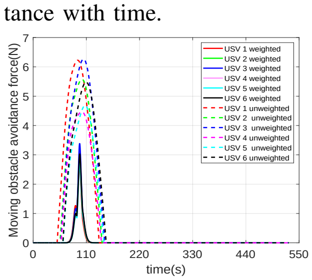

(e) Moving object and USV interaction force with time.

Figure 8: Simulation result for $n = 6$ robots, $t_r = 2$, on a collision course with a moving obstacle showing reduced cross track error with the adaptively weighted potential framework.

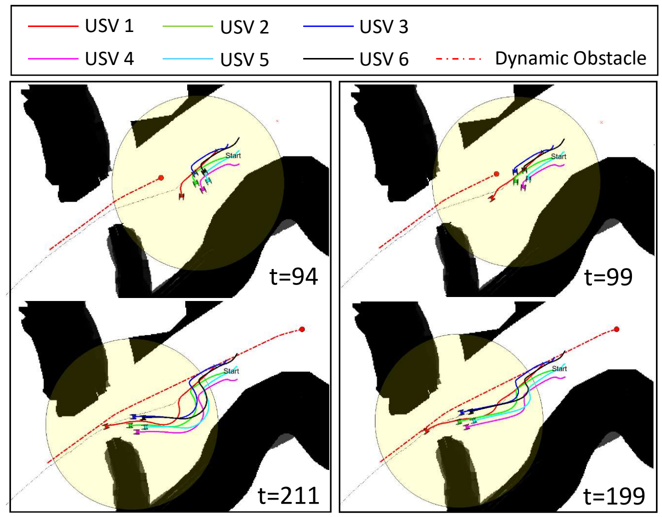

(i) Unweighted, t_r=8 (ii) Adaptively weighted, t_r=8

(a) Time lapse comparison for unweighted and adaptively weighted potential function based path following and obstacle avoidance.

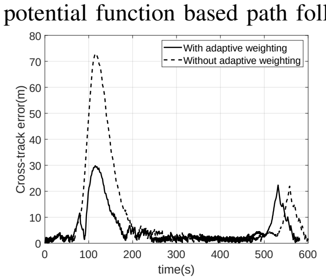

(b) Cross-track error comparison with time.

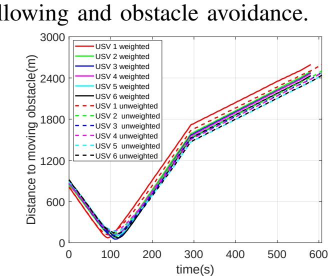

(c) USV to moving object distance with time.

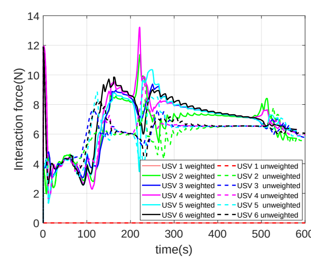

(d) Inter-agent interaction force with time.

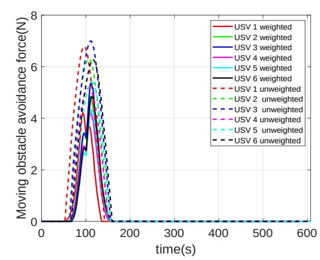

(e) Moving object and USV interaction force with time.

Figure 9: Simulation result for $n = 6$ robots, $t_r = 8$, on a collision course with a moving obstacle showing reduced cross track error with the adaptively weighted potential framework.

the proposed method as it adaptively weights the potential terms based on the moving object distance, in comparison to the unweighted framework. Simulation results of 3 and 6 USV teams with one leader having fast and slow maneuvering response times at separate instances validate reduced cross track error with the proposed adaptively weighted framework in comparison to an unweighted framework.

The significance of the proposed method in this paper is its applicability on a wide variety of USVs with different maneuvering abilities to improve dynamic obstacle avoidance and path following performance without complex dynamical model and control considerations for specific models of USVs. This generalized approach was formulated based on simple point mass dynamics and the process is continuous over time. Further work on including environment conditions such as sea surface and hydrodynamic effects, and moving object path uncertainty and prediction into the adaptively weighted potential function framework and along with experimental implementation of the system is currently underway.

VI. Acknowledgment

Yogang Singh was supported in part by the Arequipa Nexus Institute.

References

[1] X. Cao, D. Zhu, and S. X. Yang, "Multi-auv target search based on bioinspired neurodynamics model in 3-d underwater environments," *IEEE transactions on neural networks and learning systems*, vol. 27, no. 11, pp. 2364–2374, 2016.

[2] E. Fiorelli, N. E. Leonard, P. Bhatta, D. A. Paley, R. Bachmayer, and D. M. Fratantoni, "Multi-auv control and adaptive sampling in monterey bay," *IEEE journal of oceanic engineering*, vol. 31, no. 4, pp. 935–948, 2006.

[3] B. E. Bishop, "Design and control of platoons of cooperating autonomous surface vessels," in *Proc. 7th Annual Maritime Transportation System Research and Technology Coordination Conference*, 2004, pp. 1–11.

[4] T. Balch and R. C. Arkin, "Behavior-based formation control for multirobot teams," *IEEE transactions on robotics and automation*, vol. 14, no. 6, pp. 926–939, 1998.

[5] Z. Cao, L. Xie, B. Zhang, S. Wang, and M. Tan, "Formation constrained multi-robot system in unknown environments," in *2003 IEEE International Conference on Robotics and Automation (Cat. No. 03CH37422)*, vol. 1. IEEE, 2003, pp. 735–740.

[6] J. P. Desai, J. Ostrowski, and V. Kumar, "Controlling formations of multiple mobile robots," in *Proceedings. 1998 IEEE International Conference on Robotics and Automation (Cat. No. 98CH36146)*, vol. 4. IEEE, 1998, pp. 2864–2869.

[7] H. Takahashi, H. Nishi, and K. Ohnishi, "Autonomous decentralized control for formation of multiple mobile robots considering ability of robot," *IEEE Transactions on Industrial Electronics*, vol. 51, no. 6, pp. 1272–1279, 2004.

[8] M. Dorigo and L. M. Gambardella, "Ant colony system: a cooperative learning approach to the traveling salesman problem," *IEEE Transactions on evolutionary computation*, vol. 1, no. 1, pp. 53–66, 1997.

[9] D. T. Pham, A. Ghanbarzadeh, E. Koç, S. Otri, S. Rahim, and M. Zaidi, "The bees algorithm—a novel tool for complex optimisation problems," in *Intelligent Production Machines and Systems*. Elsevier, 2006, pp. 454–459.

[10] Y. Q. Chen and Z. Wang, "Formation control: a review and a new consideration," in *2005 IEEE/RSJ International conference on intelligent robots and systems*. IEEE, 2005, pp. 3181–3186.

[11] W. Guanghua, L. Deyi, G. Wenyan, and J. Peng, "Study on formation control of multi-robot systems," in *2013 Third International Conference on Intelligent System Design and Engineering Applications*. IEEE, 2013, pp. 1335–1339.

[12] H. Oh, A. R. Shirazi, C. Sun, and Y. Jin, "Bio-inspired self-organising multi-robot pattern formation: A review," *Robotics and Autonomous Systems*, vol. 91, pp. 83–100, 2017.

[13] Y. Liu and R. Bucknall, "A survey of formation control and motion planning of multiple unmanned vehicles," *Robotica*, vol. 36, no. 7, pp. 1019–1047, 2018.

[14] F. Beser and T. Yildirim, "Colregs based path planning and bearing only obstacle avoidance for autonomous unmanned surface vehicles," *Procedia computer science*, vol. 131, pp. 633–640, 2018.

[15] L. Cao and Q. Chen, "Cooperative path planning for multi-USV based on improved artificial bee colony algorithm," in *MIPPR 2017: Remote Sensing Image Processing, Geographic Information Systems, and Other Applications*, ser. Society of Photo-Optical Instrumentation Engineers (SPIE) Conference Series, vol. 10611, Mar. 2018, p. 106111G.

[16] Y. Liu and R. Bucknall, "Path planning algorithm for unmanned surface vehicle formations in a practical maritime environment," *Ocean Engineering*, vol. 97, pp. 126–144, 2015.

[17] N. A. Manzini, "Usv path planning using potential field model," Naval Postgraduate School Monterey United States, Tech. Rep., 2017.

[18] S. Xie, P. Wu, Y. Peng, J. Luo, D. Qu, Q. Li, and J. Gu, "The obstacle avoidance planning of usv based on improved artificial potential field," in *2014 IEEE International Conference on Information and Automation (ICIA)*. IEEE, 2014, pp. 746–751.

[19] X. Lin and Y. Liu, "Research on multi-usv cooperative search method," in *2019 IEEE International Conference on Mechatronics and Automation (ICMA)*. IEEE, 2019, pp. 2012–2018.

[20] W. Chao, M. Feng, W. Qing, and W. Shuwu, "A situation awareness approach for usv based on artificial potential fields," in *2017 4th International Conference on Transportation Information and Safety (ICTIS)*. IEEE, 2017, pp. 232–235.

[21] A. Motwani, "A survey of uninhabited surface vehicles," *Marine and Industrial Dynamic Analysis, School of Marine Science and Engineering, Plymouth University, Tech. Rep*, 2012.

[22] V. Bertram, "Unmanned surface vehicles-a survey," *Skibsteknisk Selskab, Copenhagen, Denmark*, vol. 1, pp. 1–14, 2008.

[23] W. Naeem, R. Sutton, and J. Chudley, "Modelling and control of an unmanned surface vehicle for environmental monitoring," in *UKACC International Control Conference*, 2006, pp. 1–6.

[24] W. Naeem, T. Xu, R. Sutton, and A. Tiano, "The design of a navigation, guidance, and control system for an unmanned surface vehicle for environmental monitoring," *Proceedings of the Institution of Mechanical Engineers, Part M: Journal of Engineering for the Maritime Environment*, vol. 222, no. 2, pp. 67–79, 2008.

[25] J. E. Manley, A. Marsh, W. Cornforth, and C. Wiseman, "Evolution of the autonomous surface craft autocat," in *OCEANS 2000 MTS/IEEE Conference and Exhibition. Conference Proceedings (Cat. No. 00CH37158)*, vol. 1. IEEE, 2000, pp. 403–408.

[26] M. Caccia, G. Bruzzone, and R. Bono, "Modelling and identification of the charlie2005 asc," in *2006 14th Mediterranean Conference on Control and Automation*. IEEE, 2006, pp. 1–6.

[27] C. A. Goudey, T. Consi, J. Manley, M. Graham *et al.*, "A robotic boat for autonomous fish tracking," *Marine Technology Society. Marine Technology Society Journal*, vol. 32, no. 1, p. 47, 1998.

[28] G. Thirunavukkarasu, L. Patrick, B. Champion, L. Chua, V. T. Huynh, and M. Joordens, "Design and development of a low-cost autonomous surface vehicle," in *2017 12th System of Systems Engineering Conference (SoSE)*. IEEE, 2017, pp. 1–6.

[29] C. Almeida, T. Franco, H. Ferreira, A. Martins, R. Santos, J. M. Almeida, J. Carvalho, and E. Silva, "Radar based collision detection developments on usv roaz ii," in *Oceans 2009-Europe*. Ieee, 2009, pp. 1–6.

[30] R. Halterman and M. Bruch, "Velodyne hdl-64e lidar for unmanned surface vehicle obstacle detection," in *Unmanned Systems Technology XII*, vol. 7692. International Society for Optics and Photonics, 2010, p. 76920D.

[31] Y. Singh, S. Sharma, R. Sutton, D. Hatton, and A. Khan, "A constrained a* approach towards optimal path planning for an unmanned surface vehicle in a maritime environment containing dynamic obstacles and ocean currents," *Ocean Engineering*, vol. 169, pp. 187–201, 2018.

[32] Z. Li and Y. Jia, "Aggregation of multi-agent systems with group leaders," *CAAI Transactions on Intelligent Systems*, vol. 1, no. 2, pp. 26–30, 2006.